Simulation numérique de la propagation d'ondes de choc en géométrie complexe par une méthode de type Galerkin Discontinu

B. Tripathi[a], R. Marchiano[a], S. Baskar[b] et F. Coulouvrat[a]
[a]Institut Jean le Rond d'Alembert-UPMC, 4 place Jussieu, 75005 Paris, France
[b]Indian Institute of Technology, Bombay, powai, 400076 Mumbai, Inde
bharat.tripathi25@gmail.com

La simulation numérique de la propagation d'ondes de choc acoustiques dans des milieux ayant une géométrie complexe est un sujet ouvert. Pourtant, un tel outil de simulation numérique serait précieux pour mieux appréhender des phénomènes tels que le bang sonique et son interaction avec la topographie, le Buzz Saw Noise ou encore la propagation d'ondes de choc résultant de traumatisme. La méthode numérique de « Galerkin discontinue » semble être une voie prometteuse. Cette méthode permet d'obtenir des schémas à la fois adaptés aux géométries complexes (car basés sur des maillages non structurés) mais aussi étant d'ordre élevé ce qui garantit une très faible dispersion et atténuation numériques, deux qualités absolument nécessaires pour la propagation en acoustique. Cependant, la prise en compte des discontinuités, associées ici aux ondes de chocs, fait l'objet de nombreuses recherches dans les différentes communautés utilisant cette méthode. Plusieurs stratégies existent comme le filtrage, l'introduction de limiteur de pente ou encore l'addition de viscosité numérique. Ces méthodes sont examinées dans le contexte de l'acoustique non linéaire.

1 Introduction

Acoustics is primarily about small amplitude perturbations, and consequently, nonlinear effects seldom get importance. But, there are instances where nonlinear terms can give rise to significant changes and play an important role in many real situations. For example, in acoustical shock waves, the nonlinearities get predominant because of long-term accumulation of small nonlinear perturbations, these are modeled by the inviscid Burgers' equation.

We choose Runge-Kutta discontinous Galerkin (RKDG) method for numerically solving such equations, as it incorporates the geometrical flexiblity of the finite element methods and the high potential of parallelization from the finite volume methods. The development of RKDG and its extension to multidimensional systems is done in a series of papers by Cockburn and Shu using hyperbolic conservation laws [1, 2, 3, 4, 5]. A similar treatment can be found for the equation of nonlinear elastodynamics in heterogeneous solid medium which are written in conservative form and then solved using DG method in [15].

During the propagation of nonlinear waves, numerical oscillations (precisely, Gibbs phenomenon) appear due to the truncation of high frequency components. Thus, these oscillations (see Fig.1) are purely numerical and do not occur physically. Consequently, the solution has to be stabilized. This is achieved by the use of various techniques namely, slope limiters, filters and the method of artificial viscosity. In this work, we develop a DG solver for the inviscid Burgers' equation as in section 2. The shock generated during the propagation is treated using the various slope limiters and the artificial viscosity terms as discussed in section 3 and section 4 respectively. The use of artificial viscosity terms in the original system generates a convection-diffusion type system, to solve we illustrate the construction of local discontinous Galerkin in section 5. The numerical results and the respective discussion is put in section 6. In section 7, we give a two-dimensional system in conservative form equivalent to the kuznetsov equation of nonlinear acoustics [7]. Finally, we end the discussion by giving the conclusions and future perspectives of this work.

2 DG Solver for Inviscid Burgers' Equation

The Burgers' equation is the simplest equation to model a one-dimensional, nonlinear problem in acoustics. In this section, we develop the DG implementation using the weak formulation of the inviscid Burgers' equation, i.e.

$$u_t + f(u)_x = 0 \tag{1}$$

where $f = \frac{u^2}{2}$, with the initial condition, $u(x,0) = u_0(x),\ x \in \mathbb{R}$. The computational domain $\Omega = [a,b]$ is partitioned as, $\Omega^k = [x_{k-1}, x_k],\quad k = 1,\cdots,N$, where N is the number of elements. We map each Ω^k onto a reference element ($I \in [-1,1]$) (for details see [8]), and the corresponding weak formulation for the reference element becomes

$$\frac{\Delta x_k}{2}(U_t, l_i) + l_i F|_{-1}^{1} - \int_{-1}^{1} F l_i'(\xi) d\xi = 0., \quad i = 0,1,\ldots,P. \tag{2}$$

where, U is the approximate solution of degree P, F is the flux, l_i are the Lagrange interpolating polynomials and $(\cdot,\cdot)$ is the standard inner product in $L^2(\Omega^k)$.

In the DG method, in order to keep the connectivity of the flux with the neighbouring elements, the flux $F|_{-1}^{1}$ at the element boundaries is replaced by F^* called the numerical flux. Applying the Legendre-Gauss quadrature, we get

$$\frac{dU_i}{dt} + \frac{2}{\Delta x_k}\left[F^*(1)\frac{l_i(1)}{w_i} - F^*(-1)\frac{l_i(-1)}{w_i} + \sum_{s=0}^{P} F_s \hat{D}_{is}\right] = 0, \tag{3}$$

where $\hat{D}_{is} = -\frac{D_{si} w_s}{w_i}$. The equation (3) is the semi-discretization of the equation (1). The flux (F) inside the element is computed using the definition of f. The numerical boundary flux (F^*) is computed using Godunov's flux for Burgers' equation as in [12]. Finally for the temporal advancement, we use the third-order low-storage Runge-Kutta method as discussed in [13].

Figure 1 shows the initial condition and the DG simulation of a period of sine-wave just after the shock formation ($L = 0.31$). The solution develops some spurious oscillations at the discontinuity which disqualifies the scheme. This outlines the need for more advanced method to counter these oscillations which are not observed physically and are purely numerical artifacts.

3 Slope Limiters

In this section, we discuss the most common slope limiters used for reducing the spurious oscillations at the discontinuties or shocks produced in propagation of nonlinear waves. Here we illustrate three slope limiters, namely, the first by Cockburn *et al.* [2], the second by Biswas *et al.* [9] as a modification of the first one, and the third an extension of Biswas given by Burbeau *et al.* [10].

We have computed the approximate solution in *nodal form* i.e. where the solution is written as a Lagrange

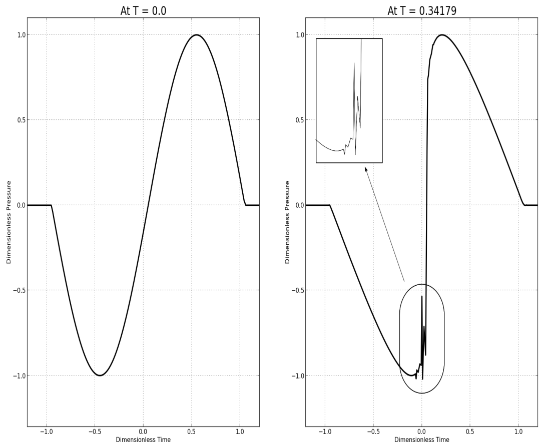

FIGURE 1 – Waveform obtained after the propagation of a period of a sine-wave (left) beyond shock length (right) ($L = 0.31$)

interpolant of degree P. Alternatively, the approximate solution can be represented in *modal form* where the solution is written as a sum of P orthogonal Legendre polynomials [13]. The two forms are represented as

$$x \in \Omega^k \;:\; u_h^k(x,t) \;=\; \sum_{n=0}^{P} \hat{u}_n^k(t) P_n(x), \qquad (4)$$

$$x \in \Omega^k \;:\; u_h^k(x,t) \;=\; \sum_{i=0}^{P} u_h^k(x_i^k, t) l_i^k(x). \qquad (5)$$

Here, $P_n(x)$ are the Legendre polynomials of degree n, $l_i^k(x)$ are the Lagrange interpolating polynomials and $u_h^k(x,t)$ is the approximate solution in the kth element of size h. Also, equation (4), can be written in matrix form as

$$\mathcal{V}\hat{\boldsymbol{u}} = \boldsymbol{u}, \text{ where } \mathcal{V}_{ij} = P_{j-1}(\xi_i), \;\; \xi_i \in [-1,1]. \qquad (6)$$

Quoting [8], the matrix $\mathcal{V}$ is recognized as the generalized *Vandermonde* matrix and will play a key role in development of the scheme. For implementing the slope limiters, we need the modes ($\hat{\boldsymbol{u}}$), which can be achieved using (6) as $\hat{\boldsymbol{u}} = \mathcal{V}_{ij}^{-1}\boldsymbol{u}$.

We start with the slope limiter given by Cockburn *et al.* [2]. It modifies the boundary flux for each element and consequently new modal values are computed. As a result, the new limited solution is generated using these new modal values. This flux limiter conserves the monotonocity of the average solution i.e. $\hat{u}_0^k(t)$. Here, we define

$$\begin{aligned} \widetilde{u_k} &= u_h^k(1,t) - \hat{u}_0^k(t) = \textstyle\sum_{n=1}^{P} \hat{u}_n^k(t) P_n(1), \\ \widetilde{\widetilde{u_k}} &= u_h^k(-1,t) - \hat{u}_0^k(t) = \textstyle\sum_{n=1}^{P} \hat{u}_n^k(t) P_n(-1) \end{aligned} \qquad (7)$$

For the sake of brevity, we drop the argument t from the modes in the following equations. We modify $\widetilde{u_k}$ and $\widetilde{\widetilde{u_k}}$ as

$$\widetilde{u_k}^{new} = \text{minmod}\left(\widetilde{u_k}, \hat{u}_0^{k+1} - \hat{u}_0^k, \hat{u}_0^k - \hat{u}_0^{k-1}\right),$$

$$\widetilde{\widetilde{u_k}}^{new} = \text{minmod}\left(\widetilde{\widetilde{u_k}}, \hat{u}_0^k - \hat{u}_0^{k+1}, \hat{u}_0^{k-1} - \hat{u}_0^k\right)$$

respectively, where

$$\text{minmod}(a_1, \cdots, a_n) = \begin{cases} \text{sign}(a_1) \min\limits_{1 \le i \le n} |a_i|, & \text{if} \quad \text{sign}(a_1) = \cdot \\ & \qquad\quad \cdot = \text{sign}(a_n) \\ 0, & \qquad\quad \text{otherwise} \end{cases}$$

Now, for $P = 2$ the new modes $\hat{u}_1^{k(new)}$ and $\hat{u}_2^{k(new)}$ can be uniquely determined by solving the linear system,

$$\begin{aligned} \widetilde{u_k}^{new} &= \hat{u}_1^{k(new)} P_1(1) + \hat{u}_2^{k(new)} P_2(1), \\ \widetilde{\widetilde{u_k}}^{new} &= \hat{u}_1^{k(new)} P_1(-1) + \hat{u}_2^{k(new)} P_2(-1) \end{aligned} \qquad (8)$$

But for $P \geq 3$, the modes can no longer be uniquely determined using these modified fluxes. If the modes, $\hat{u}_1^{k(new)}$ and $\hat{u}_2^{k(new)}$ turn out to be different from the original modes then the remaining modes $n \geq 3$ are made 0.

While preserving the monotonocity of the average numerical solution, this slope limiter flattens the smooth extrema. To overcome this, Biswas *et al.* [9] proposed to determine the higher-order modes by limiting the solution moments. The limiter is given as follows,

$$(2n-1)\hat{u}_n^{k(new)} = \text{minmod}\Big((2n-1)\hat{u}_n^k, \hat{u}_{n-1}^{k+1} - \hat{u}_{n-1}^k, \hat{u}_{n-1}^k - \hat{u}_{n-1}^{k-1}\Big) \qquad (9)$$

As it is evident from (9), this slope limiter works adaptively i.e. it works only when it feels the need of itself. First, the highest-order coefficient is limited, then successively the lower-order coefficients are limited when the next higher order coefficient on the interval has already been changed by limiting. In this way, the limiting is applied only where it is needed, and the accuracy is retained in smooth regions.

As an extension of the previous slope limiter, Burbeau *et al.* [10] proposed this new limiter. Here, the Biswas limiter is used as a regularity criterion given by

$$(2n-1)u_n^{k(min)} = \text{minmod}\Big((2n-1)\hat{u}_n^k, \hat{u}_{n-1}^{k+1} - \hat{u}_{n-1}^k, \hat{u}_{n-1}^k - \hat{u}_{n-1}^{k-1}\Big) \qquad (10)$$

If $u_n^{k(min)} = \hat{u}_n^k$ then the limited solution will be

$$u_h^k(x,t) = \sum_{l=0}^{n} \hat{u}_l^k P_l(x) + \sum_{l=n+1}^{P} \hat{u}_n^{k(new)} P_l(x) \qquad (11)$$

or else, $\hat{u}_n^{k(new)} = \text{maxmod}\left(u_n^{k(min)}, u_n^{k(max)}\right)$ where,

$$(2n-1)u_n^{k(max)} = \text{minmod}\Big((2n-1)\hat{u}_n^k(t), w_+^k - \hat{u}_{n-1}^k(t), \hat{u}_{n-1}^k(t) - w_-^k\Big) \qquad (12)$$

$$w_+^k = \hat{u}_{n-1}^{k+1} - (2n-1)\hat{u}_n^{k+1}, \text{ and} \quad w_-^k = \hat{u}_{n-1}^{k-1} + (2n-1)\hat{u}_n^{k-1} \qquad (13)$$

$$\text{maxmod}(a_1, \cdots, a_n) = \begin{cases} \text{sign}(a_1) \max\limits_{1 \le i \le n} |a_i|, & \text{if} \quad \text{sign}(a_1) = \cdot \\ & \qquad\quad \cdot = \text{sign}(a_n) \\ 0, & \qquad\quad \text{otherwise} \end{cases} \qquad (14)$$

Here, the slopes are limited using the unlimited slopes of the neighbouring elements, and one must store the limited slopes and the unlimited slopes separately until all the limited slopes are computed.

Conclusively, the slope limiters are tools that reduces the order of the solution to the first order or less when a shock is detected. As a counterpart, they damp the smooth extrema as expected. Moreover from fig.2, we can infer that the slope limiters need a sufficiently high number of elements to work satisfactorily, as in this particular case we have $N = 200$ and $P = 3$ for the domain $[-1.2, 1.2]$. There efficiency decreases when the number of elements decreases, for instance when $N = 40$ and $P = 5$ the limiting becomes unsatisfactory (see fig.3).

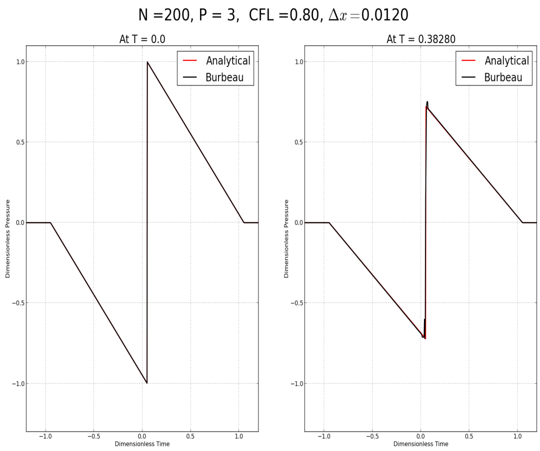

Figure 2 – The numerical solution using the limiter proposed by Burbeau *et al.* (10)-(14). Left : initial condition. Right : numerical solution compared to the analytical at time $t = 0.38$

4 Artificial Viscosity

An alternative mechanism for stablizing the shocks is the use of *artificial viscosity* terms in the considered hyperbolic system of equations. The idea behind the artificial viscosity method is to add a dissipative model term to the original hyperbolic equation. For example, the augmented one dimensional scalar hyperbolic equation looks like

$$u_t + f(u)_x = (\epsilon u_x)_x. \tag{15}$$

The right hand side term is the dissipative term added. The parameter ϵ controls the amount of viscosity, it is expected to be zero anywhere but around the shock. Therefore, a sensor is needed to detect the discontinuity. Persson *et al.* [14] came with a approach of discontinuity sensor, which is as follows.

Define,

$$u_h^k(x,t) = \sum_{i=1}^{P} \hat{u}_i P_i, \tag{16}$$

$$\tilde{u}_h^k(x,t) = \sum_{i=1}^{P-1} \hat{u}_i P_i. \tag{17}$$

Then, the Smoothness Indicator is defined as

$$S_k = \frac{(u - \tilde{u}, u - \tilde{u})_k}{(u,u)_k}. \tag{18}$$

Based on this definition, they define the artificial viscosity funtion as

$$\epsilon_k = \begin{cases} 0 & \text{if} \quad s_k < s_0 - \kappa \\ \frac{\epsilon_0}{2}\left(1 + \sin\left(\frac{\pi(s_k - s_0)}{2\kappa}\right)\right) & \text{if} \quad s_0 - \kappa \le s_k < s_0 + \kappa \\ \epsilon_0 & \text{if} \quad s_k > s_0 + \kappa \end{cases} \tag{19}$$

where, $s_k = \log_{10} S_k$ and the parameters $\epsilon_0 \approx O(\frac{h}{p})$, $s_0 \approx \log_{10} O(\frac{1}{p^4})$ and κ is chosen empirically sufficiently large so as to obtain a sharp but smooth shock profile. Note, these parameters will vary from problem to problem. Therefore, tests are to be made before fixing these parameters for a particular model. An extension of this work has been done by Klockner *et al.* [16].

Another instance is the use of continuous artificial viscosity, as can be found in Barter *et al.* [17], where the diffusion equation is used as a model for the artificial viscosity. Once the viscosity is determined using this model, they plug it in the state vector of the Navier-Stokes equation and solve the system using the DG method. Here, the shock is sensed using the smoothness indicator proposed by Persson *et al.* as in equation (18).

The problem with the use of piecewise-contant artificial viscosity function is that it induces oscillations at the boundary of the element as there is jump in the viscosity only and neither u_x nor u has jumps. In the light of this, we propose the use of a continuous smooth artificial viscosity profile, which we call as *Gaussian artificial viscosity*, is defined as

$$\epsilon(x) = \epsilon_0 \exp\left[-\left(\frac{x - x_0}{\sigma_0}\right)^2\right], \tag{20}$$

where, ϵ_0, σ_0, x_0 are chosen depending on the shock strength, shock structure and the position of the shock respectively. Instead of using the smoothness indicator (18), we propose to use the second mode ($\hat{u}_1^k$) of the modal solution (4) to sense the shock. Once the shock is sensed, the Gaussian artificial viscosity is centered around the shock position. Note, whenever the shock is detected, and only then, the viscosity becomes nonzero and the inviscid Burgers' equation (1) transforms into a convection-diffusion equation (15) with $f(u) = u^2/2$. The adaptive implementation of this idea is an interest of future work.

5 Convection-Diffusion Equation

The augmented inviscid Burgers' equation with the artificial viscosity term (15), is nothing but a convective-diffusive equation. Here, we intend to solve the equation,

$$u_t + \left(\frac{u^2}{2}\right)_x = (\epsilon(x) u_x)_x \tag{21}$$

using the Local DG method (see [6]). In this method, we need to write the equation (21) as a system of first-order equation i.e.

$$\begin{cases} u_t + \left(\frac{u^2}{2}\right)_x - (\epsilon(x) q)_x & = & 0 \\ q - u_x & = & 0 \end{cases} \tag{22}$$

or,

$$\begin{cases} u_t + (f - \epsilon(x) q)_x & = & 0 \\ q - B_x & = & 0 \end{cases} \tag{23}$$

where $f = \frac{u^2}{2}$ and $B = u$. Also, define the total flux ($\mathcal{F}$) as

$$\mathcal{F} = f - \epsilon q \tag{24}$$

In order to write the weak formulation for the first-order system (23), the Lagrange polynomials are used as the test functions. If P is the degree of polynomial interpolation, the inner mesh looks like $x_0^k, x_1^k, x_2^k, \cdots, x_{P-2}^k, x_{P-1}^k, x_P^k$.

For $x \in \Omega^k$, the approximate solution in nodal form looks like

$$u_h^k(x,t) = \sum_{i=0}^{P} u_h^k(x_i^k,t) l_i^k(x), \tag{25}$$

where h is the width of an element. The other varibles like $\mathcal{F}_h^k$, q_h^k, B_h^k can be similarly expressed in nodal form.

Consequently, the weak formulation is

$$\int_{\Omega^k} \frac{\partial u_h^k}{\partial t} l_j^k(x) dx - \int_{\Omega^k} \mathcal{F}_h^k \frac{\partial l_j^k(x)}{\partial x} dx + \left[\hat{\mathcal{F}}_h^k(x_r^k) l_j^k(x_r^k) - \hat{\mathcal{F}}_h^k(x_l^k) l_j^k(x_l^k)\right] = 0 \tag{26}$$

$$\int_{\Omega^k} q_h^k l_j^k(x) dx + \int_{\Omega^k} B_h^k \frac{\partial l_j^k(x)}{\partial x} dx - \left[\hat{B}_h^k(x_r^k) l_j^k(x_r^k) - \hat{B}_h^k(x_l^k) l_j^k(x_l^k)\right] = 0 \tag{27}$$

On substituting (25) in the above equation, we get

$$\sum_{i=0}^{P} \frac{du_h^k(x_i^k,t)}{dt} \left(l_i^k(x),\ l_j^k(x)\right) - \sum_{i=0}^{P} \mathcal{F}_h^k(x_i^k,t) \left(l_i^k(x),\ \frac{\partial l_j^k(x)}{\partial x}\right) + \left[\hat{\mathcal{F}}_h^k(x_r^k) l_j^k(x_r^k) - \hat{\mathcal{F}}_h^k(x_l^k) l_j^k(x_l^k)\right] = 0 \tag{28}$$

$$\sum_{i=0}^{P} q_h^k(x_i^k,t) \left(l_i^k(x),\ l_j^k(x)\right) + \sum_{i=0}^{P} B_h^k(x_i^k,t) \left(l_i^k(x),\ \frac{\partial l_j^k(x)}{\partial x}\right) - \left[\hat{B}_h^k(x_r^k) l_j^k(x_r^k) - \hat{B}_h^k(x_l^k) l_j^k(x_l^k)\right] = 0. \tag{29}$$

Note that the auxillary variable q_h^k will be eliminated by using the equation (29) in (28).

From (28)-(29), we identify that there are two terms of boundary fluxes i.e. $\hat{\mathcal{F}}$ and $\hat{B}$. First, we take the numerical flux $\hat{\mathcal{F}}$, which is defined as

$$\hat{\mathcal{F}} = \hat{f} - \hat{\epsilon}\hat{q}. \tag{30}$$

Here, $\hat{f}$ is defined using the *Lax-Friedrich* flux i.e.

$$\hat{f}(x^-, x^+) = \frac{1}{2}\left[f(x^-) + f(x^+) + \lambda(u(x^-) - u(x^+))\right] \tag{31}$$

where $\lambda = \max_{\inf u_h(x) < s < \sup u_h(x)} |f_u(s)|$.

For defining the fluxes $\hat{q}$ and $\hat{B}$, we use the *alternating principle* [18], which gives

$$\hat{\epsilon} = \epsilon^+,\ \hat{q} = q^+ \text{ and } \hat{B} = B(u^-) \tag{32}$$

6 Numerical Experiment

In order to have a simulation for a long duration, we need to have a sufficiently large spatial domain for the wave propagation, which is not very convenient from a computational point of view. Therefore in acoustics, we solve the problem in retarded time, i.e. when a frame of interest is chosen in the spatial domain and then travels in time at the sound speed. For this setup the Burgers' equation is

$$\frac{\partial \overline{p}}{\partial \overline{\sigma}} - \overline{p}\frac{\partial \overline{p}}{\partial \overline{\tau}} = 0, \quad \text{where } \overline{p} = \frac{p_a}{p_0}, \quad \overline{\sigma} = \frac{x}{L}, \quad \overline{\tau} = \omega_0\left(t - \frac{x}{c_0}\right). \tag{33}$$

Here, $\overline{p}, \overline{\sigma}, \overline{\tau}$ a the dimensionless pressure, distance and time (retarded) respectively. Also, ω_0 is the characteristic angular frequency of wave, and L is the characteristic distance (shock length) for the nonlinear effects. Here, we solve the equation (33) with the *sawtooth wave* as the initial condition,

$$\overline{p}(\tau, 0) = \begin{cases} -(\tau + 0.95), & \text{if} \quad -0.95 \le \tau \le 0.05 \\ -(\tau - 1.05), & \text{if} \quad 0.05 < \tau \le 1.05 \\ 0, & \text{Otherwise} \end{cases}$$

The domain of interest is $\Omega = [-1.2, 1.2]$, which is discretized in $N = 40$ elements with the order of polynomial approximations being $P = 5$. The distance of propagation is $\overline{\sigma} = 0.38$ and $CFL = 0.8$. All the numerical solutions discussed in this article i.e. the unstabilized solution (unlimited), solutions obtained using various limiters and the solution obtained using the Gaussian artificial viscosity (20) are compared with the analytical solution in fig.3. A comparison of computation times of all the methods is given in table 1.

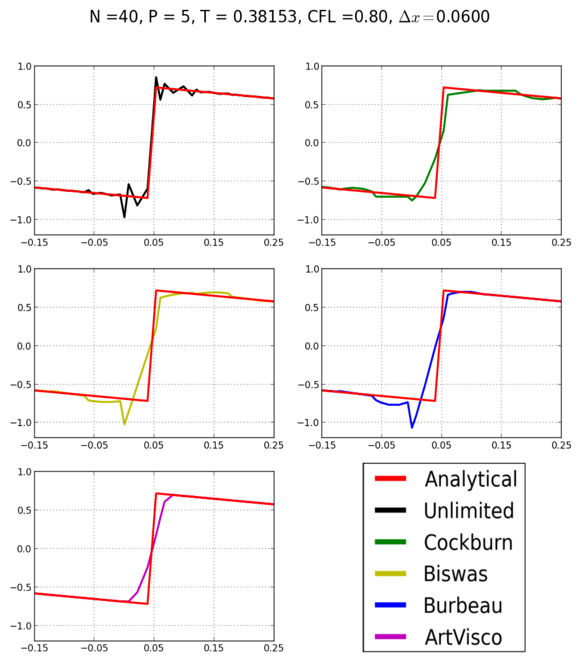

FIGURE 3 – Zoom-in around the shock showing the comparison of the unlimited solution, limited solutions and solution obtained using the Gaussian artificial viscosity (ArtVisco) with the analytical solution.

Stabilizing Method	Normalized Time Ratio
Unlimited	1.00
Cockburn	1.74
Biswas	2.44
Burbeau	4.63
ArtVisco	1.83

Tableau 1 – Comparison of Computation Time

Conclusively, as in fig.3 it can be seen that all the solutions whether limited or not, are in good agreement with the analytical solution for almost all the domain except around the discontinuity. At the discontinuity, the unlimited solution is having some spurious oscillations whereas the limited methods by Burbeau, Biswas and Cockburn show a smoothing effect. However, the solution obtained by the method of artificial viscosity turns out as the most precise even near the shock : it is the only one that shows no oscillations at all. Moreover, the computation time taken by the artificial viscosity method is comparable with the lower limit of the time taken by the slope limiters. Therefore, the method of artificial viscosity is more accurate and efficient than the limiters.

7 Extension in Two-dimensions

As a future work, we intend to extend the method to the Kuznetsov equation [7]. We start with a system of first-order equations containing the quadratic nonlinear terms equivalent to the Kuznetsov equation of nonlinear acoustics. The fluid is assumed to be homogeneous in composition and quiescent i.e. its ambient density and pressure are uniform and there is no ambient flow. Also, the viscous and thermal components are neglected. With the primary variables being expressed as the sum of ambient quantities and acoustic perturbations, for instance, $p(\boldsymbol{x},t) = p_0 + p_a(\boldsymbol{x},t)$ where, the subscript 0 and a indicates the ambient quantities and acoustic perturbations respectively. We define $\boldsymbol{v} = (u(x,y,z,t), v(x,y,z,t), w(x,y,z,t))$ as the fluid velocity, ρ is the fluid density, p is the pressure, U is the internal energy and E is the total energy. Using this setup, we give

$$\frac{\partial \rho_a}{\partial t} + \nabla\cdot(\rho_0 \boldsymbol{v}_a + \rho_a \boldsymbol{v}_a) = 0. \tag{34}$$

$$\begin{bmatrix} \rho(\boldsymbol{x},t)u_a \\ \rho(\boldsymbol{x},t)v_a \\ \rho(\boldsymbol{x},t)w_a \end{bmatrix}_t + \nabla\cdot\begin{bmatrix} \rho_0 u_a^2 + p(\boldsymbol{x},t) & \rho_0 v_a u_a & \rho_0 w_a u_a \\ \rho_0 u_a v_a & \rho_0 v_a^2 + p(\boldsymbol{x},t) & \rho_0 w_a v_a \\ \rho_0 u_a w_a & \rho_0 v_a w_a & \rho_0 w_a^2 + p(\boldsymbol{x},t) \end{bmatrix} = 0, \tag{35}$$

$$\frac{\partial E}{\partial t} + \nabla\cdot[\boldsymbol{v}_a(E + p(\boldsymbol{x},t))] = 0 \tag{36}$$

where,

$$E = \tfrac{1}{2}\rho(\boldsymbol{x},t)\boldsymbol{v}_a^2(\boldsymbol{x},t) + \rho(\boldsymbol{x},t)U(\boldsymbol{x},t) \ ,$$

Here, $p_a(x,t)$ is determined using the state equation i.e.

$$p_a(x,t) = c_0^2 \rho_a^2 \tag{37}$$

This set of equations can be used to derive the Kuznetsov equation with just algebraic manipulations and without any additional assumption. Note, the system is of first-order equations in conservative form, therefore it would be an extension of Burgers' equation to multidimensional system.

8 Conclusions and Perspectives

In this work, we infer that the use of artificial viscosity is more accurate and is computationally more efficient than the slope limiters. In future, we would extend the method of artificial viscosity to the system of equations for nonlinear acoustics in two-dimensions .

9 Acknowledgments

This work has been accomplished under project (No. 4601-1) funded by CEFIPRA (Indo-French Centre for the Promotion of Advance Research) and partially aided by EGIDE (Campus France).

Références

[1] B. Cockburn and C.-W. Shu , The Runge-Kutta local projection P^1-discontinuous Galerkin finite element method for scalar conservation laws, *IMA Preprint Series-388*, (1988)

[2] B. Cockburn and C.-W. Shu , TVB Runge-Kutta local projection discontinuous Galerkin finite element method for conservation laws II : general framework, *Math. Comput.* **52**, 411-435 (1989)

[3] B. Cockburn, S.-Y. Lin and C.-W. Shu, TVB Runge - Kutta local projection discontinuous Galerkin finite element method for conservation laws III : one dimensional system, *J. Comput. Phys.* **84**, 90-113 (1989)

[4] , B. Cockburn, S. Hou and C.-W. Shu, Runge - Kutta local projection discontinuous Galerkin finite element method for conservation laws IV : the multidimensional case, *Math. Comput.* **54**, 545-581 (1990)

[5] B. Cockburn and C.-W. Shu , The Runge-Kutta discontinuous Galerkin method for conservation laws V : multidimensional system, *J. Comput. Phys.* **141**, 199-224 (1998)

[6] B. Cockburn, and C.-W. Shu, The local discontinuous Galerkin method for time-dependent convection-diffusion systems,*SIAM J. Numer. Anal.* **35**, 2440-2463 (1998)

[7] V. P. Kuznetsov ; Equation of Nonlinear Acoustics In *Sov. Phys. Acous.* **16-4**,467-470 (1971).

[8] J. S. Hesthaven and T. Warburton ; *Nodal Discontinuous Galerkin methods : Algorithm, Analysis and Applications* Springer (2008).

[9] R. Biswas, K. D. Devine and J. E. Flaherty ; Parallel, adaptive finite element methods for conservation laws In *Appl. Numer. Math.* **14**,255-283 (1994).

[10] A. Burbeau, P. Sagaut, and Ch.-H. Bruneau ; A Problem-Independent Limiter for High-order Runge-Kutta Discontinuous Galerkin Methods In *J. of Comput. Phy.* **169**,111-150 (2001).

[11] E. Casoni, J. Peraire and A. Huerta ; One-dimensional shock-capturing for high-order discontinuous Galerkin methods In *Int. J. Numer. Meth. Fluids* **71**,737-755 (2013).

[12] B. Van Leer, On the relation between the upwind-differencing schemes of Godunov, Engquist-Osher and Roe. In *SIAM J. Sci. Stat. Comput.* **5** (1984)

[13] D.A. Kopriva, *Implementing Spectral Methods for Partial Differential Equations*, Springer (2009)

[14] P.-O. Persson and J. Peraire, Sub-Cell Shock Capturing for Discontinous Galerkin Methods, *Collection of Technical Papers-44th AIAA Aerospace Sciences Meeting* **2**, 1408-1420 (2006)

[15] O. B. Matar, P.-Y. Guerder, Y. Li, B. Vandewoestyne and K. V. D. Abeele, A nodal discontinuous Galerkin finite element method for nonlinear elastic wave propagation, *J. Acoust. Soc. Am.* **131-5**, 3650-3663 (2012)

[16] A. Klockner, T. Warburton and J. S. Hesthaven, Viscous Shock Capturing in a Time-Explicit Discontinous Galerkin Method, *Math. Model. Nat. Phenom.* **10**, 1-27 (2011)

[17] G.E. Barter and D.L. Darmofal, Shock capturing with PDE-based artificial viscosity for DGFEM : Part I. Formulation, *J. Comput. Phys.* **229**, 1810-1827 (2010)

[18] J. Yan and C.-W. Shu, Local Discontinuous Galerkin Method for Partial Differential Equations with Higher Order Derivatives, *J. Sci. Comput.* **17**,(2002)